ELSEVIER

Thin Solid Films 306 (1997) 198–204

thin solid films

Structural characterization of self-assembled quantum dot structures by X-ray diffraction techniques

A.A. Darhuber [a,*], J. Stangl [a], V. Holy [a,1], G. Bauer [a], A. Krost [b], M. Grundmann [b], D. Bimberg [b], V.M. Ustinov [c], P.S. Kop'ev [c], A.O. Kosogov [d], P. Werner [d]

[a] *Institut für Halbleiterphysik, Universität Linz, A-4040 Linz, Austria*
[b] *Institut für Festkörperphysik, TU-Berlin, D-10623 Berlin, Germany*
[c] *A.F. Ioffe Physical-Technical Institute, 194021 St. Petersburg, Russian Federation*
[d] *Max-Planck-Institut für Mikrostrukturphysik, D-06120 Halle, Germany*

Abstract

We have investigated, by means of X-ray diffraction reciprocal space mapping and X-ray reflectivity, multilayers of self-organized InGaAs quantum dots grown on GaAs by MBE. An anisotropy of the average inter-dot spacings in the [100] and [110] directions was found, consistent with an ordering of the dots in a two-dimensional square lattice with main axes along the $< 100 >$-directions and a lattice parameter of 55 nm. The nearly perfect vertical alignment (stacking) of the dots was deduced consistently from the diffraction peak shape and from measurements of the resonant diffuse scattering in the X-ray reflection regime. © 1997 Elsevier Science S.A.

Keywords: X-ray diffraction; Self-assembled quantum dots; Reciprocal space mapping

1. Introduction

Quantum well structures in which a one-dimensional potential $V(z)$ restricts the quasi-free motion of mobile carriers into two dimensions are widely used in electronic and optoelectronic devices. Quantum wire or quantum dot structures, in which the electron motion is further confined either in two or in all three dimensions, offer interesting prospects for devices, in particular for lasers with low threshold currents. The traditional method for fabrication of such low-dimensional structures relies on the growth of heterostructures by molecular beam epitaxy (MBE) or chemical vapor deposition (CVD), and the subsequent lateral constriction of the electron motion either by gates, or by lithography in conjunction with etching techniques. However, the controlled nanofabrication with such techniques suffers the draw-back that quite often passivated layers underneath the free surfaces are created, caused by the damage introduced during the nanolithography processes. This effect is detrimental from the point of view of actual device applications.

Thus, during the past years, there has been an increasing interest in using stresses already present in heteroepitaxial systems as driving forces for nanostructure formation. Such stresses at heterostructure interfaces can lead to a three-dimensional growth mode, favoring the appearance of strained islands, thereby relieving at least partially the built-in heteroepitaxial strain [1–4]. The important advantage of this approach to nanofabrication is the fact that the damage and the contamination from the above-mentioned lateral patterning techniques are avoided.

Whereas for the growth of quantum well structures one aims at a two-dimensional layer by layer growth mode, the Stranski–Krastanow growth regime can be exploited for the growth of self-assembled dot structures in systems where the epilayer has a larger lattice constant than the substrate (e.g. InAs on GaAs, Ge on Si, etc.). In this growth mode, first a two-dimensional wetting layer is formed up to a certain thickness, above which the growth mode changes to a three-dimensional one. The islands which are formed are coherent with respect to the layers underneath, i.e. no dislocations nucleate up to a certain limit. For the realization of lasers, a high dot density is

* Corresponding author.
[1] Permanent address: Dept. of Solid State Physics, Masaryk University, Brno, Czech Republic.

PII S0040-6090(97)00097-7

required which can be achieved by growing dot-multilayers.

An inherent problem in the preparation of self-organized quantum dots is the statistical distribution of size and position of the individual dots. Although considerable effort has been spent on the optimisation of the growth parameters in order to narrow the size distribution, the statistical fluctuations still keep photoluminescence lines broad. The homogeneity of the island size depends on the strain energies involved, which can induce a limiting island size [1].

An interesting possibility for a further reduction of these size fluctuations has been proposed and demonstrated by Tersoff et al. [2], who have stacked many single layers resulting in a dot-superlattice. It is known from TEM investigations that stacked dots show a more or less perfect vertical alignment, owing to the strain fields which extend into the barrier material [3,4]. In Ref. [2] a theoretical model was presented which not only accounted for this nearly perfect vertical correlation, but which also predicted a reduction of the statistical size-fluctuations if several dot layers are stacked. Moreover, the correlation of the lateral dot positions in the top layers increases compared to that of a single dot layer. The arrangement of islands is not simply reproduced from layer to layer, but there is a tendency for a more uniform island size and spacing with an increasing number of layers.

For the study of these phenomena, quite often cross-section transmission electron microscopy (TEM) has been used, a technique which requires (destructive) sample preparation procedures. Furthermore, atomic force microscopy for probing the surface morphology has been employed, which cannot be used directly for the investigation of samples with cap layers (which are, however, necessary for devices like lasers). For these reasons another non-destructive technique for the investigation of multilayers is necessary. In this paper we will show that useful information on multilayer dot structures, e.g., vertical and horizontal correlations and strain fields, can be obtained by X-ray diffraction techniques.

2. Experimental

In this paper we will restrict ourselves to the investigation of GaInAs dot multilayers by high-resolution X-ray diffraction and X-ray reflectivity techniques. The multilayers with 20 and 25 periods of nominally 1.2 nm $In_{0.5}Ga_{0.5}As$ dot layers and GaAs barriers with a thickness of 5 nm have been grown on (001)-oriented GaAs substrates by molecular beam epitaxy (MBE). Above and below the dot-superlattices, GaAs buffer layers and AlGaAs/GaAs short period superlattices have been deposited. The growth temperature was varied between 450 °C and 600 °C. Additional details of the growth process can be found in Ref. [5]. Schmidt et al. [6] have studied the optoelectronic properties of InAs quantum dot lasers fabricated from similar samples, which operate at room temperature as well [7].

The X-ray diffraction measurements have been performed with a Philips MRD laboratory diffractometer (at a wavelength of 1.54 Å). The MRD is equipped with a four-crystal Ge (220) monochromator and a channel-cut Ge (220) analyzer, which guarantee an angular resolution of 12 arc sec and a monochromaticity of $\Delta\lambda/\lambda = 1 \times 10^{-4}$. The independent variation of the two diffraction angles ω (between the primary X-ray beam and the sample surface) and 2θ (between incident and diffracted X-ray waves) provides the possibility of reciprocal space mapping, i.e. two-dimensionally resolved measurements of distributions of diffracted X-ray intensity. X-ray reflection measurements have been performed at the OPTICS-beamline of ESRF, Grenoble, and the D4-beamline of HASYLAB, Hamburg.

3. Transmission electron microscopy

Transmission electron microscopy (TEM) investigations revealed the shape of the dots as flat-top pyramids with base lengths along the $< 100 >$ directions of about 18 nm and heights around 5 nm. Fig. 1 shows a cross-section high-resolution transmission electron micrograph giving information on the dot shape and its evolution with increasing number of dot layers. In Fig. 2 we have depicted a cross-section TEM micrograph ((002) dark field image, incident beam direction parallel to $< 110 >$) of the 25 period sample. The nearly perfect vertical alignment ('stacking') of the islands is clearly visible. The GaAs–

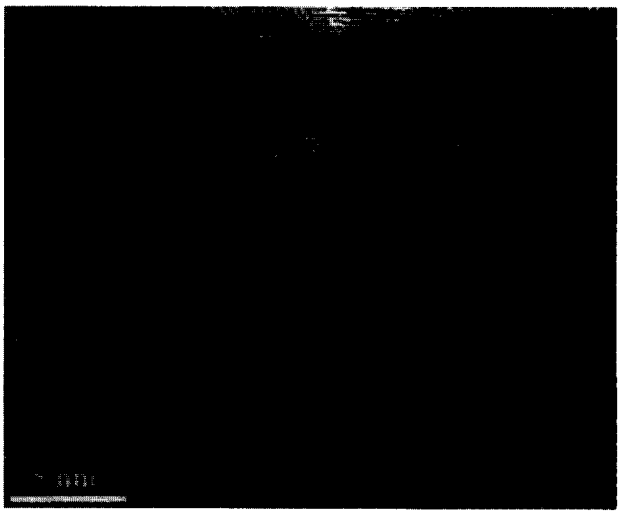

Fig. 1. High-resolution transmission electron micrograph of the 25 period sample.

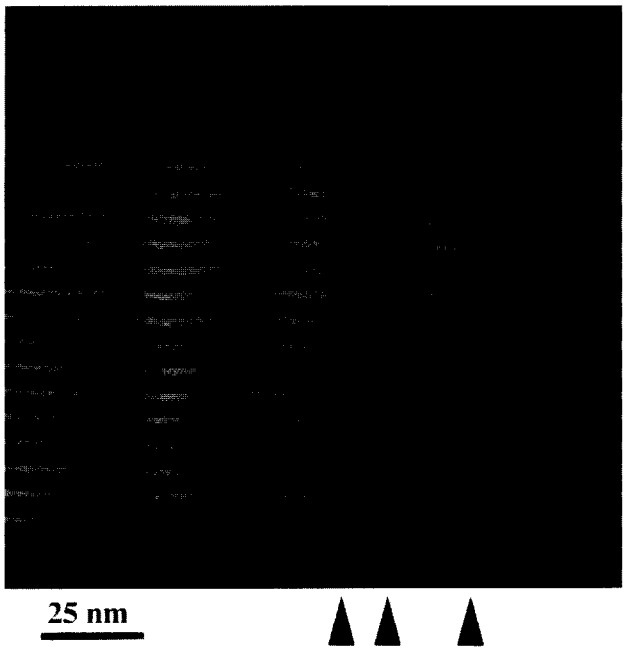

Fig. 2. Transmission electron micrograph of the 25 period sample.

GaInAs interfaces become rather wavy at the top of the structure.

4. X-ray diffraction and reflectivity

The multilayer periodicity of the 20 and 25 period samples manifests itself in conventional rocking curves as a series of superlattice (SL) satellites (Fig. 3). The sharp SL peaks are due to the two-dimensional GaInAs wetting layers embedded in the GaAs layers. These narrow extrema are superimposed on rather broad peaks (see, e.g., the SL_{-1} satellite in Fig. 3), which stem from the dots. More precisely, the dots give rise to a diffusively scattered intensity distribution, which is integrated in 2θ direction in the double crystal diffraction geometry used. In order to separate the contributions from the dots and the wetting layers as much as possible, two-dimensional reciprocal space maps (RSM's) were recorded. For Bragg diffraction

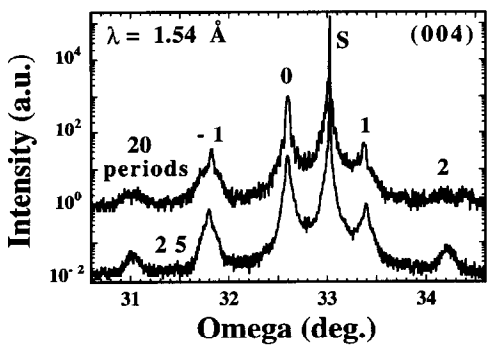

Fig. 3. (004) rocking curves of the 20 and 25 period samples.

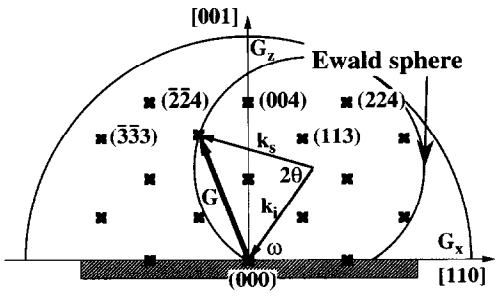

Fig. 4. Sketch of the reciprocal lattice and the diffraction geometry.

and [001]-growth direction, we have sketched the Ewald sphere in reciprocal space for a certain scattering geometry in Fig. 4, where the reciprocal plane is determined by q_z parallel to [001]- and q_x parallel to the [110]-direction. In this orientation the RSMs around the (004), (224) and (113) reciprocal lattice points were acquired. For the RSM around the (404) reflection, q_x is parallel to the [100]-direction. The (004) map usually exhibits a sharp coherent peak and some diffuse scattering around it, but no pronounced signatures of the dots. If the angle of incidence of the X-rays is reduced to a few degrees around (113), (224) and (404), the coherence length of the X-rays (several μm) increases by a factor of 3 to 10 and the sensitivity to lateral ordering is enhanced.

The (224) RSM of the multilayer sample with 20 periods consists of a sharp coherent peak (labelled 'C' in Fig. 5a) underneath the substrate peak and a broad diffuse satellite peak (labelled 'D' in Fig. 5a), which we ascribe to the occurrence of lateral ordering. This is substantiated by the (113) RSM, where the spacing between coherent peak and the satellite peak is identical within experimental accuracy. Thus the satellite peak is due to a lateral length

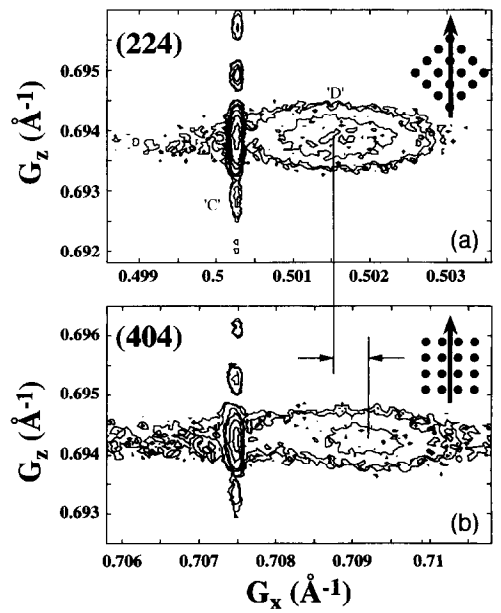

Fig. 5. (224) and (404) reciprocal space map.

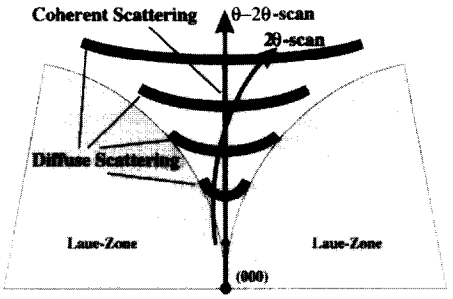

Fig. 6. Sketch of the intensity distribution and the applied scan types in the reflectivity regime around (000).

scale and not to e.g. strain relaxation. The dot spacing deduced from the peak separation is approximately 78 nm in the [110] direction.

A very interesting feature appeared in the (404) map (Fig. 5b), which is measured under an azimuth of 45° relative to the (224)-orientation (i.e. the sample is rotated around the surface normal by 45°). The peak spacing increased by approximately a factor of $\sqrt{2}$, corresponding to a decrease of the inter-dot distance to approximately 55 nm. Thus, our results are consistent with an ordering of the dots in a square lattice with main axes parallel to $< 100 >$ and a lattice constant of approximately 55 nm.

The dot spacing in the TEM-micrograph of Fig. 2 is considerably smaller because of the finite thickness of the TEM-specimen. If the islands are aligned along $< 100 >$-directions and projected onto a (110)-plane, only every second column of islands may be used for the evaluation of the dot-spacing in the (110)-plane under consideration.

We have studied the vertical correlation of the dots in these multilayer samples by X-ray reflectivity measurements at the Hasylab D4- and the Optics-beamline at the ESRF Grenoble. The scattering geometry is shown in Fig. 6. The coherently scattered radiation from the two-dimensional InGaAs wetting and GaAs spacer layers is measured with a θ–2θ scan. Interface undulations give rise to diffuse scattering. For vertically correlated undulations, this diffuse scattering has broad maxima beside the coherent SL satellites (see Fig. 6). Their FWHM in the q_z-direction is a measure of the range of vertical correlation (i.e. the smaller this FWHM the better the correlation), which can be assessed by a 2θ-scan in reciprocal space (see Fig. 6). Such a scan intersects the coherent θ–2θ scan at a certain point, and crosses the banana-shaped diffuse scattering maxima.

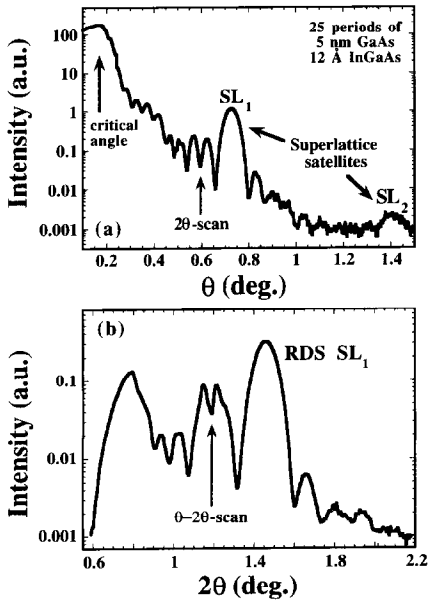

Fig. 7. Specular 2θ-scan (a) and θ–2θ-scan (b) of the 25 period sample.

Experimental data for these two types of scans through the reciprocal lattice are shown in Fig. 7, recorded for the 25 period sample. In the specular scan the maxima denoted by SL_1 and SL_2 stem from the GaAs/GaInAs multilayer structure, the further subsidiary extrema reflect the complicated layer sequence. A 2θ-scan for an incidence angle of 0.6 degrees ($\lambda = 1.05$ Å) is shown in Fig. 7b. The coherent reflection pattern around SL_1 of Fig. 7a is indeed perfectly reproduced in the diffuse scattering recorded in Fig. 7b, which proves the nearly perfect vertical correlation.

5. Theoretical model and analysis

We have performed simulations of the reciprocal space maps to gain an understanding of the diffraction patterns using kinematical X-ray diffraction theory. It turned out that the far field of the elastic relaxation, which can be approximated by the deformation field of anisotropic point defects, is the essential part for the intensity distribution around the 0th-order superlattice-peak. The three-dimensional strain distribution in and around the pyramid-shaped InGaAs dots has been calculated numerically as described in Ref. [8]. These near-field deformations (Fig. 8a and b) influence the diffraction pattern at the higher-order satellites.

X-ray diffraction from an arrangement of self-assembled quantum dots is influenced by the strains inside and outside the dots as well as by the shape of these islands and their relative positions. The theoretical description is restricted to the diffuse maxima, since the coherent peaks do not yield any information on the dots. The diffuse scattering is investigated in the vicinity of the SL_0 with the diffraction vector $\boldsymbol{h}$ defined with respect to the mean crystal structure of the MQW. The intensity is expressed as a function of $\boldsymbol{q} = \boldsymbol{Q} - \boldsymbol{h}$, where $\boldsymbol{Q} = \boldsymbol{k}_{out} - \boldsymbol{k}_{in}$ is the momentum transfer vector.

The deformation inside the dots is determined by the elastic relaxation of the lattice mismatch. Its distribution in the dots is involved and depends on the elastic properties of InGaAs and GaAs, and on the geometrical shape of the

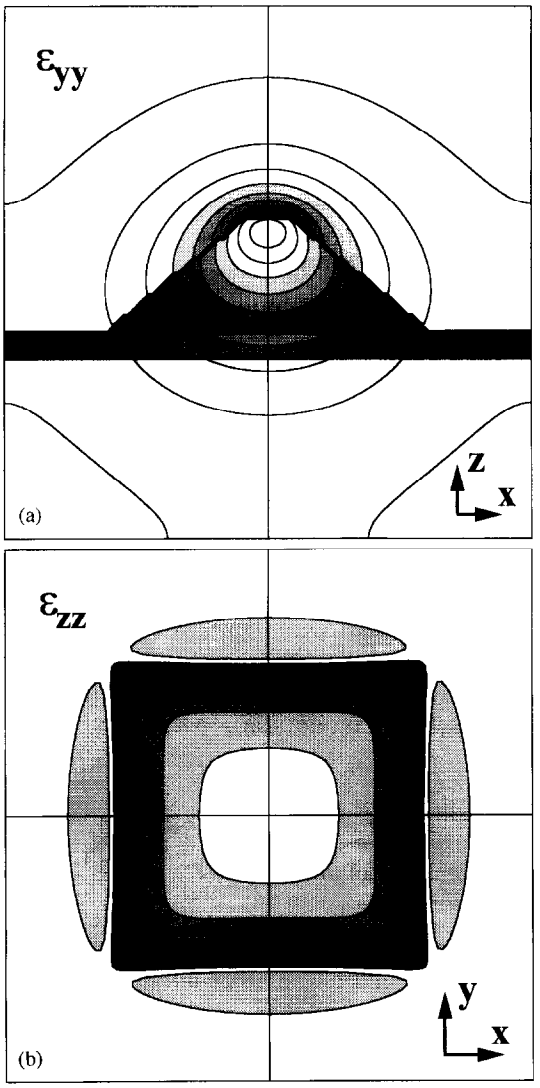

Fig. 8. Finite differences calculation of the strain fields in and around the dots. (a) ϵ_{yy} in the central xz-plane (contours ranging from -0.03 to 0.02), (b) ϵ_{zz} in the center of the wetting layer (contours from 0.012 to 0.04). The calculated area is approx. 23×23 nm^2.

islands. For simplicity we assume that the strain tensor ϵ inside the dot has constant elements expressing the misfit of the two lattices. If $2\pi/|\boldsymbol{q}|$ is much larger than the size of the dots, the deformation field outside the dots can be replaced by the asymptotic deformation field of a dot far from its center [9]. This asymptotic deformation field can be well approximated by the one spherical inclusion. The strain is also influenced by the elastic relaxation of the internal stresses at the free surface of the sample. The deformation field $\boldsymbol{t}(\boldsymbol{r};Z)$ of an isotropic defect lying at the depth Z below the free surface has been calculated in Ref. [10].

The positional distribution of the islands in the individual periods of the multilayer is described by the statistical distribution function $c(\boldsymbol{R})$ (unity if position $\boldsymbol{R}$ is occupied by a dot, else zero). The correlation function of this lateral and vertical distribution w is defined as $w(\boldsymbol{R},\boldsymbol{R}') = <c(\boldsymbol{R})c(\boldsymbol{R}')>$. The dots are lying in planes with distances $Z_n = nD$ $(n = 0 \ldots N)$ below the free surface, where D is the multilayer period and N the total number of dot layers. Since the sample is (statistically) homogeneous, the correlation function $w(\boldsymbol{R}_\parallel,\boldsymbol{R}'_\parallel;Z_n,Z_m)$ depends only on the difference of the lateral coordinates $w = w_{nm}(\boldsymbol{R}_\parallel - \boldsymbol{R}'_\parallel;Z_n,Z_m)$, where $\boldsymbol{R}_\parallel = (X,Y,0)$ is the in-plane component of the position vector $\boldsymbol{R}$ of the dot.

Since we concluded from the experimental RSMs (Fig. 2) that the dot centers lie in a disordered orthogonal grid with the main axes along the $<100>$-crystallographic axes, the two-dimensional correlation function $w_{nn}(\boldsymbol{R}_\parallel - \boldsymbol{R}'_\parallel)$ is a product of two one-dimensional correlation functions: $w_{nn}(\boldsymbol{R}_\parallel - \boldsymbol{R}'_\parallel) = w_{nn}(X-X')w_{nn}(Y-Y')$. Furthermore, the correlation function $w_{n\neq m}$ is assumed in the form of a weighted average of the correlated and uncorrelated components:

$$w_{nm}(\boldsymbol{R}_\parallel - \boldsymbol{R}'_\parallel) = w_{nn}(\boldsymbol{R}_\parallel - \boldsymbol{R}'_\parallel)\left[p_v + (1-p_v)\delta_{nm}\right] + \langle c(\boldsymbol{R})\rangle^2(1-\delta_{nm})(1-p_v), \quad (1)$$

where p_v is the fraction of vertically correlated (stacked) dots (i.e. a perfect vertical correlation corresponds to $p_v = 1$). The 2nd term of this expression does not depend on the lateral coordinates, and therefore it only contributes to a central δ-like peak of the Fourier transformation of w^{FT}, which is essential for the calculation of the scattered intensity. Although the lateral correlation is improved with increasing number of multilayers [2], we will assume – for the sake of simplicity – that the statistical parameters of the in-plane distribution of the islands do not depend on the index n of the individual periods and thus $w_{nn} = w_\parallel$.

On the basis of the deformation field of the dots and their statistical distribution we can calculate the dependence of the diffusely scattered intensity on $\boldsymbol{q}$. The calculation is based on the kinematical theory of diffuse X-ray scattering [9,11]. From this theory the following formula for the diffusely scattered intensity can be deduced:

$$\begin{aligned} I(q_x,q_z) &= p_v A\int_{-\infty}^{\infty} \mathrm{d}q_y\, w_{nn}^{FT}(\boldsymbol{q}_\parallel)|F_1 H(\mathrm{i}q_z) + F_2 H(-q_\parallel)|^2 \\ &\quad + (1-p_v)A\int_{-\infty}^{\infty} \mathrm{d}q_y\, w_{nn}^{FT}(\boldsymbol{q}_\parallel) \\ &\quad \times\left[N|F_1|^2 + |F_2|^2 H(-2q_\parallel) \right. \\ &\quad \left. + 2\mathrm{Re}\left(F_1 F_2^* H(\mathrm{i}q_z - q_\parallel)\right)\right], \end{aligned} \quad (2)$$

where $\boldsymbol{q}_\parallel$ is the in-plane projection of $\boldsymbol{q}$, and A is a constant. Here we have denoted

$$F_1 = \mathrm{i}\chi_{hL}\Phi_\infty(\boldsymbol{q}) + \chi_{hD}\Omega^{FT}(\boldsymbol{q}+\epsilon\boldsymbol{h}) - \chi_{hL}\Omega^{FT}(\boldsymbol{q})$$
$$\text{and } F_2 = 2\chi_{hL}\Phi(\boldsymbol{q}), \quad (3)$$

and $H(p) = \sum_{n=0}^{N}\exp(pnD)$ is the geometrical factor of the multilayer. $\Omega(\boldsymbol{r})$ is the shape function of a dot (unity

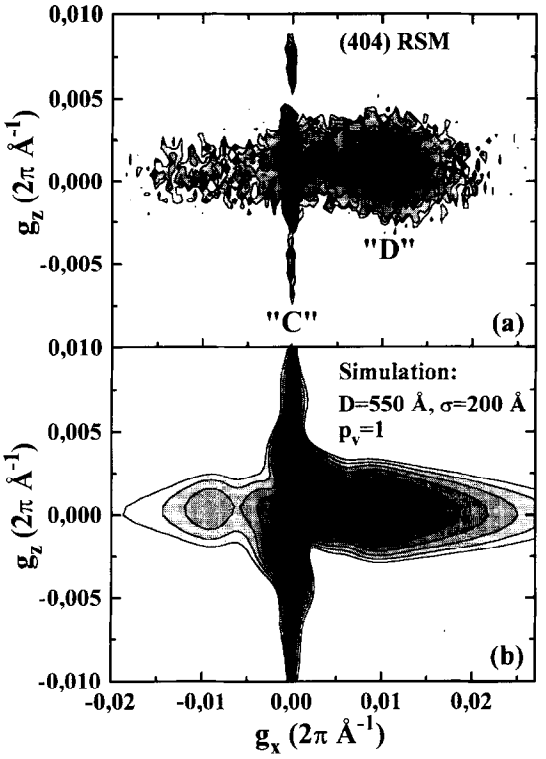

Fig. 9. Measured (a) and simulated (b) (404) RSM.

inside the dot, zero outside of it), Ω^{FT} is its Fourier transformation, χ_{hL} and χ_{hD} are the polarizabilities of the crystal and the dot, respectively. $\Phi_\infty(q)$ is the Fourier transformation of $h.t_\infty(r)$, $t_\infty(r)$ is the deformation field of a defect in an infinite isotropic continuum. The second term $\Phi(q)$ reflects the influence of the surface and its exact form can be found in Ref. [11]. The integration over the y-component of q (perpendicular to the scattering plane) is due to low resolution of the diffractometer in this direction. Additional details of the theory will be published elsewhere [12].

The measured and simulated (404) maps for the 20 period sample are shown in Fig. 9a and b. Hence, the features of the measurement are well reproduced qualitatively. The center of mass of the diffracted intensity is on the right-hand side of the coherent maximum as in the experimental map. Although the peak at the left-hand side of the coherent maximum is not visible in the measurement in Fig. 9a (because of the insufficient counting statistics due to the low diffracted intensity), it appears as a pronounced shoulder in the integrated maps (not shown here).

Another result of the simulations (deduced from the FWHM of the dot peak in the q_z-direction) is that the dots are highly correlated in the vertical direction ($p_v \approx 0.95$), which is well known from TEM observations [3,4] (see Fig. 1). It is also in perfect agreement with synchrotron X-ray reflection measurements of our samples in particular of the non-specular resonant diffuse scattering originating in the dot superlattice. As shown in Ref. [13], such investigations yield information on both the lateral and vertical correlations of interface undulations of multilayers.

The standard deviation of the lateral dot-distance distribution was determined from the simulations as 20 nm; thus a lateral positional correlation extends over just a few islands.

Grazing incidence diffraction experiments on uncovered single layers of Ge-hut clusters grown on (001)-oriented Si were reported by Williams et al. [14] and Steinfart et al. [15], who derived the lateral strain in the Ge-islands as well.

6. Conclusions

We have studied multiple layers of self-assembled InGaAs dots by means of high-resolution X-ray diffraction and reflection. A lateral self-ordering of the dots – as predicted theoretically [2] – was deduced from reciprocal space maps. Moreover, evidence for an anisotropy of the inter-dot spacing along the [100]- and [110]-directions has been found, consistent with the ordering of the dots in a square lattice with a lattice parameter of 55 nm along the $< 100 >$-directions. The degree of vertical correlation has been determined consistently in a non-destructive way from both X-ray diffraction and reflectivity.

Acknowledgements

X-ray reflection measurements have been performed at the OPTICS-beamline at ESRF and the D4-beamline of HASYLAB. The assistance of Alexej Souvorov and Holger Rhan is gratefully acknowledged. This work has been supported by the FWF-project No. 10083, by the Austrian BMWVK and by the GME.

References

[1] J. Drucker, Phys. Rev. B 48 (1993) 18203.
[2] J. Tersoff, C. Teichert, M.G. Lagally, Phys. Rev. Lett. 76 (1996) 1675.
[3] L. Goldstein, F. Glas, J.Y. Marzin, M.N. Charasse, G. Le Roux, Appl. Phys. Lett. 47 (1985) 1099.
[4] Q. Xie, A. Madhukar, P. Chen, N.P. Kobayashi, Phys. Rev. Lett. 75 (1995) 2542.
[5] M. Grundmann, N.N. Ledentsov, R. Heitz, L. Eckey, J. Christen, J. Böhrer, D. Bimberg, S.S. Ruvimov, P. Werner, U. Richter, J. Heydenreich, V.M. Ustinov, A.Yu. Egorov, A.E. Zhukov, P.S. Kopév, Zh.I. Alferov, Phys. status solidi 188 (1995) 249.
[6] O.G. Schmidt, N. Kirstaedter, N.N. Ledentsov, M.-H. Mao, D. Bimberg, V.M. Ustinov, A.Y. Egorov, A.E. Zhukov, M.V. Maximov, P.S. Kop'ev, Z.I. Alferov, Electron. Lett. 32 (1996) 1302.
[7] N.N. Ledentsov, Proc. 23rd Int. Conf. on the Physics of Semiconductors (ICPS-23), Berlin, July 1996, (World Scientific, Singapore).
[8] M. Grundmann, O. Stier, D. Bimberg, Phys. Rev. B 52 (1995) 11969.

[9] P.H. Dederichs, Phys. Rev. B 4 (1971) 1041.
[10] V.B. Molodkin, S.I. Olikhovski, M.E. Osinovski, Phys. Metals 5 (1984) 1.
[11] M.A. Krivoglaz, X-ray and Neutron Diffraction in Non-Ideal Crystals, Springer, Berlin, 1996.
[12] A.A. Darhuber, P. Schittenhelm, V. Holy, J. Stangl, G. Bauer, G. Abstreiter, Phys. Rev. B, in press.
[13] V. Holy, T. Baumbach, Phys. Rev. B 49 (1994) 10668.
[14] A.A. Williams, J.M.C. Thornton, J.E. Macdonald, R.G. van Silfhout, J.F. van der Veen, M.S. Finney, A.D. Johnson, C. Norris, Phys. Rev. B 43 (1991) 5001.
[15] A.J. Steinfort, P.M. Scholte, A. Ettema, F. Tuinstra, M. Nielsen, E. Landemark, D.M. Smilgies, R. Feidenhans'l, G. Falkenberg, L. Seehofer, R.L. Johnson, Phys. Rev. Lett. 77 (1996) 2009.